Chemical Engineering Journal 162 (2010) 406–414

Contents lists available at ScienceDirect

Chemical Engineering Journal

journal homepage: www.elsevier.com/locate/cej

Novel NiZr-based porous biomaterials: Synthesis and *in vitro* testing

Khachatur Manukyan[a,d,*], Narine Amirkhanyan[a], Sofiya Aydinyan[a], Vardan Danghyan[a], Ruzanna Grigoryan[b], Natalia Sarkisyan[b], Gennadi Gasparyan[b,c], Rouben Aroutiounian[c], Suren Kharatyan[a,d]

[a] Department of Inorganic Chemistry, Yerevan State University, 1 Manoogian Str, Yerevan 0025, Armenia
[b] Group of Cytology, Institute of Molecular Biology NAS of Armenia, 7 Hasratyan Str, Yerevan 0014, Armenia
[c] Department of Genetics and Cytology, Yerevan State University, 1 Manoogian Str, Yerevan 0025, Armenia
[d] Laboratory of Kinetics of SHS Processes, A.B. Nalbandyan Institute of Chemical Physics NAS of Armenia, 5/2 Sevak Str, Yerevan 0014, Armenia

ARTICLE INFO

Article history:
Received 3 December 2009
Received in revised form 9 May 2010
Accepted 20 May 2010

Keywords:
NiZr biomaterial
Combustion synthesis
Porosity
Cytotoxicity
Genotoxicity

ABSTRACT

Novel porous NiZr-based potential biomaterials for orthopaedic application were developed using the combustion reaction in the Ni + Zr + additive mixtures. The effect of various additives (ZrH_2, $CaCO_3$, NH_4F and Teflon) on the combustion behaviour in the low-caloric Ni + Zr mixtures was investigated. To obtain molten porous NiZr-based product Teflon was chosen as an optimal additive. Combustion conditions of the Ni + Zr + Teflon mixtures depending on various factors were investigated. NiZr-based materials with 55–65% porosity and 50–550 μm pore sizes were obtained. The cyto- and genotoxicity of the materials was tested *in vitro* using HeLa and KCL-22 cell lines. After several extractions the obtained porous materials expressed no toxicity. Produced materials were non-genotoxic and had no effect on the cell proliferation.

1. Introduction

Today there is a great need in long-term biomaterials for reconstructive medicine [1–4]. A list of requirements to these materials is impressive [5]. Briefly, mechanical properties of such biomaterials should match those of the tissue at the site of implantation; materials should be biocompatible to match cell/tissue growth and should not provoke adverse host responses. For load-bearing orthopaedic applications, metals (alloys) have so far shown the greatest potential as the basis for scaffolds owing to their excellent mechanical strength and resilience when compared to alternative biomaterials, such as polymers and ceramics [1–3]. Metal bone substitutes are also necessary to mimic the tissue architecture (to be highly porous with an interconnected pore network) to provide osteocyte ingrowth and flow transport of nutrients and metabolic waste. The appropriate pore size is shown to be 100–500 μm [1,4].

There have been numerous efforts to develop porous alloys with the proper characteristics [1]. Many existing metallic biomaterials (e.g., plasma-sprayed titanium, porous sintered powder metallurgy materials), however, do not easily lend themselves to fabrication into porous structures [4,6].

For the last decades, new ZrNb-based biomaterials (e.g., Oxinium) attract attention as they combine the proper balance of mechanical properties and corrosion resistance with excellent biocompatibility [6–8]. However, application of ZrNb-based alloys as porous bone scaffolds is limited [4,6] because of difficulties to manufacture porous ZrNb refractory alloys (the eutectic is about 1750 °C) [9]. Fabrication-related difficulties may be overcome if niobium is replaced with more ductile metals such as nickel or cobalt. In such a way the melting point of alloys may be reduced from 1850 °C (melting point of zirconium) down to 960 °C (the deepest eutectic point) [9]. As zirconium remains the major component of alloys, their corrosion resistance is believed will not be affected significantly.

A current challenge in manufacturing of intermetallic biomaterials is the development of simple and non-traditional synthesis methods providing required characteristics of products. Recently, the combustion synthesis (CS) technique [1,10,11] has been applied to produce novel biomaterials. The CS process utilizes heat generated by an exothermic reaction to sustain itself in the form of a combustion wave after external local ignition. The attractive features of CS are the high temperatures (1000–3000 °C) and short reaction times (s) [10,11]. As a practical alternative to sintering, conventional powder metallurgical processing and alloy development technologies, CS has several advantages, including low energy requirements, the simplicity of experimental device used, chemical homogeneity and high purity of the products (due to gas and

* Corresponding author at: Yerevan State University, 1 Manoogian Str, Yerevan 0025, Armenia, Tel.: +374 10 28 16 10; fax: +374 10 28 16 34.
E-mail address: khachat@ichph.sci.am (K. Manukyan).

1385-8947/$ – see front matter © 2010 Elsevier B.V. All rights reserved.
doi:10.1016/j.cej.2010.05.042

Table 1
Precursors used.

Precursors	Trademark	Particle size (μm)
Zirconium powder	PZrK-1 (Tech. condition of manufacturing 48-4-234-76 of the Russian Standards Agency)	5–10
Zirconium powder	PZrK-1 (Tech. condition of manufacturing 48-4-234-76 of the Russian Standards Agency)	150–200
Nickel powder	PNE-1 (High grade, Norilsk Nickel, Russia)	<10
ZrH_2	Combustion synthesized, in-house made, hydrogen content 2.0 wt.%	<10
$CaCO_3$	Mikhart-2, Provencale, France	<8
NH_4F	High grade (St. Petersburg Factory of Chemical Reagents)	5–10
Teflon $(C_2F_4)_n$	FT-4 (High grade, UralXimPlast, Nizhnii Tagil, Russia)	<10

volatile impurities' evolution originated by high heating rate and temperatures developed in the combustion wave) and its ability to be scaled-up.

To date, some commonly accepted and novel potential materials for biomedical applications including porous NiTi [12–16], NiTi–TiC and Ni_3Ti–TiC [17–19], tricalcium phosphate [17] or hydroxyapatite [20], pore-free CoCrMo [21] and Ti-based multicomponent coatings [22] are successfully prepared using CS technologies. The CS process in NiTi intermetallic alloys was studied in details [12–16] according to the following reaction:

$$Ni + Ti \rightarrow NiTi + 67\,kJ\,mol^{-1}$$

This system needs preheating of initial reagent mixtures (to 300–600 °C) because of relatively low temperature of the reaction between Ni and Ti. The existence of pores in the initial samples (about 30–40%), the transient liquid phase, the volatilisation of impurities and adsorbed gases contribute to obtaining products with the final porosity as high as 55–65%.

To avoid the procedure of preheating it is possible to use additives able to develop simultaneous highly exothermic reaction. It was shown [17–19], particularly, that adding of graphite into the Ni + Ti mixture increases overall thermal effect of the process enabling to fabricate Ni_3Ti–TiC and NiTi–TiC potential biomaterials. Ammonium fluoride was also demonstrated to stimulate combustion processes in many reacting systems [23,24]. Effect of Teflon as a chemical activator of the CS in various low-caloric systems was earlier revealed by us [25–28].

A feasible way to fabricate porous intermetallic alloys by CS reaction is supplementing of gasifying agents to the reaction mixture. Earlier the application of Ca_3N_2 and $CaCO_3$ to control the structure of Ni_3Ti–TiC and NiTi–TiC alloys has been reported [17,19]. Transition metals hydrides (e.g., TiH_2) have been also used to produce porous Ti-based intermetallics [25,29].

Therefore, development of comprehensive combustion-based technology to stimulate both synthesis process and *in situ* gas generation to favour pore formation is of special interest.

The toxicological profile of new materials is of critical importance for their biocompatibility evaluation. In modern toxicological research, testing of cyto- and genotoxicity *in vitro* (in cell cultures) is widely used to predict acute and chronic toxicity of new compounds and materials *in vivo* [30,31].

The objectives of the present work are the fabrication of NiZr-based materials by chemically activated CS technique and the study of some features (composition and morphology, porosity, cyto- and genotoxicity) of obtained materials that are known to influence the host response to biomaterials [5].

2. Materials and methods

2.1. Synthesis of materials

The following reaction system was investigated in this study:

$$[(100-\alpha)\%Ni + \alpha\%Zr] + \beta\%\ additive$$

where α and β are the ratios (in wt.%) of reactants and additives, respectively.

The raw mixtures were prepared using materials listed in Table 1. Fine (5–10 μm) and coarse-grained (150–200 μm) zirconium powders as well as fine (less than 10 μm) powders of nickel and additives ($CaCO_3$, NH_4Cl, Teflon and ZrH_2) were used as precursors. They were mixed at desired ratio in a ceramic mortar for at least 1 h. Then the mixtures were cold-pressed in a stainless

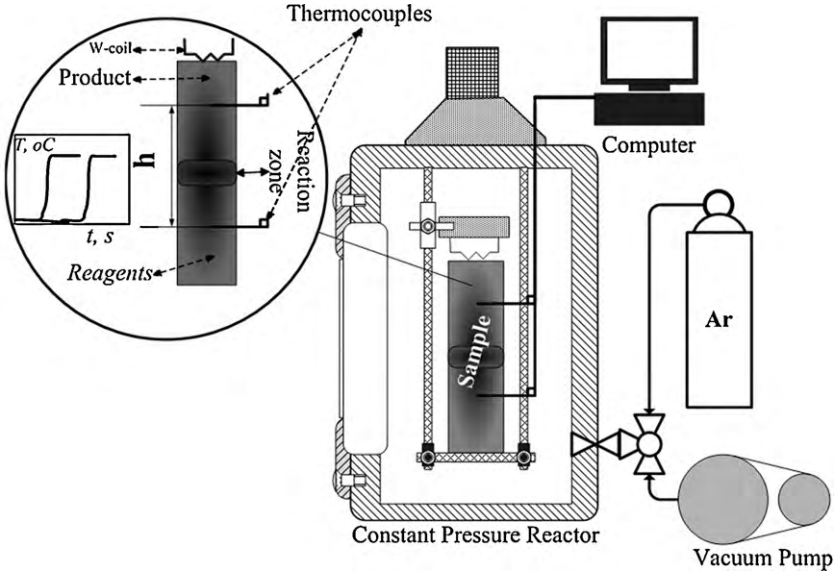

Fig. 1. Experimental setup.

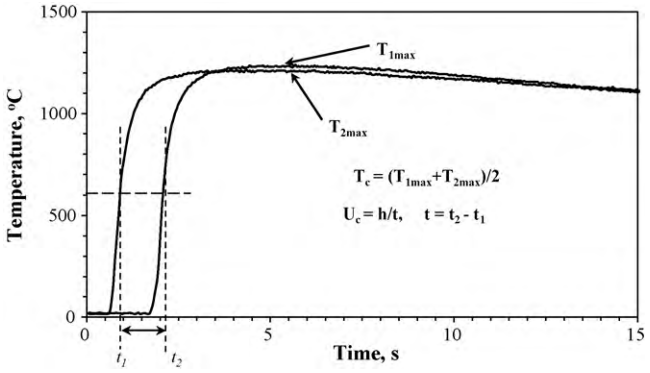

Fig. 2. Typical temperature-time distribution of the combustion process.

steel uniaxial die (diameter 20 mm) to produce uniform cylindrical samples with the bulk density in the range 2.0–2.5 g cm^{-3}.

Experiments were conducted in a setup (Fig. 1) containing the laboratory constant pressure reactor CPR-3l (Sapphire Co, Armenia) in argon atmosphere (purity 99.8%, oxygen content no more than 0.1%) at pressures 0.1–1 MPa. Samples were placed into the reactor, it was sealed, evacuated, purged with inert gas for three cycles and filled with argon to the desired pressure. The combustion process was initiated by means of a tungsten coil positioned above the upper surface of sample and was programmed to produce a voltage pulse 12–18 V for 1–2 s. The coil supply with power was automatically discontinued after ignition of a sample.

2.2. Measurements of combustion parameters

The maximum combustion temperature (T_c) and the temperature distribution (Fig. 2) through the combustion wave were measured by tungsten-rhenium thermocouples (W/Re-5 and W/Re-20, 100 μm in diameter) covered with a thin layer of boron nitride. Two thermocouples were put into holes (diameter 2 mm, depth 10 mm) drilled beforehand in each specimen perpendicularly to the cylinder axis at ~1 cm interval (see Fig. 1). The output signals of thermocouples were transformed by a data acquisition system at the rate of 2 kHz and were recorded by a computer. The average value of combustion velocity (U_c) was calculated as follows: $U_c = h/t$, where h is a distance between thermocouples; $t = t_2 - t_1$ is the time distance between thermocouple signals (Fig. 2). The values of t_1 and t_2 were taken for the half of the maximum combustion temperature (T_{max}) for each thermocouple. The standard error of measurements for T_c and U_c were ±15 °C and 5%, respectively.

2.3. Characterization of additives and products

The general porosity (π) of the product was calculated by the formula:

$$\pi = \left(1 - \frac{\rho}{\rho_o}\right) \times 100,$$

where ρ is the specimen density as a weight/volume ratio and ρ_o is its theoretical density calculated from the starting composition using the rule of mixtures. The density of a specimen was determined by measuring its weight and dimensions.

The microstructural analysis was carried out by scanning electron microscopy (Tesla BS 300, Czech Republic) of samples previously polished with silicon carbide paper and diamond paste. Pore size distribution was estimated by quantitative image analysis software Image-Pro Plus.

For XRD analysis by DRON-3.0 diffractometer (Burevestnik, Russia) with monochromatic CuKα radiation the obtained materials were crushed to fine powders.

Differential thermal analysis (DTA) and differential thermogravimetry (DTG) of additives and initial mixtures were performed in argon flow using "Derivatograph Q1500" (MOM, Hungary). Heating rate at the DTA experiments was adjusted to 20 K min^{-1}.

In order to determine the existence, concentrations, and composition of water-soluble impurities, the materials were washed and the ion contents were determined in the extracts. To this end pieces of samples (diameter 20 mm, thickness 2.5–4 mm) were washed with deionised water (3–4 g of materials per 100 ml of water) for four days at 40 °C with everyday changing of water. Extracts obtained from the first and forth extractions were analyzed by ELAN-9000 ICP-Mass-Spectrometer and Dionex ICS-1000 chromatograph system to determine the concentration of cations (Fe, Zn, Cu, Ni, Zr, *etc.*) and anions (F^-, NO_3^-, *etc.*).

2.4. In vitro testing of materials' cytotoxicity

The cell lines used were HeLa (human cervix carcinoma, monolayer) and KCL-22 (human chronic myeloid leukemia, suspension). Cells were routinely maintained in the growth medium RPMI-1640 (Sigma–Aldrich) supplemented with 10% fetal bovine serum (Biochrom AG, Germany) and 50 μg ml^{-1} gentamycin (Belmedpreparaty, Belarus) at 37 °C.

The cytotoxicity of materials was tested with the vital dye (trypan blue) exclusion test [32]. This method is based on the principle that viable cells do not take up the dye, whereas cells with compromised cell membrane integrity (dead ones) do. The trypan blue test is known to overestimate the number of viable cells, but this technique is sufficient for comparative studies. Briefly, fluid extracts of materials tested were obtained by placing heat sterilized (180 °C for 2 h) pieces of materials in separate growth media under standard conditions (0.2 g ml^{-1} of the medium for 24 h at 37 °C). Each extract obtained was then applied to the cultures grown for two days, replacing the medium that had nourished the cells to that point. In this way, cells were supplied with a fresh medium containing extractables derived from the materials. The cultures were then incubated for 72 h and viable cell number was counted by the vital dye exclusion test. Attached HeLa cells were previously suspended with trypsin–EDTA (Sigma–Aldrich). Cell viability was expressed as a percentage of intact controls. At least quadruplicate cultures were scored for an experimental point.

To follow the dynamics of release of materials' extractable components into the medium the same pieces of materials were used sequentially in a series of four experiments. Three of them were performed using HeLa cells, and KCL-22 cells were used in the fourth experiment as this cell line was shown earlier to be very sensitive to toxic compounds [33].

2.5. In vitro estimation of materials' genotoxicity and cell cycle effects

To determine the genotoxicity of alloys the cytokinesis-block variant of the *in vitro* micronucleus (MN) test [34–37] was applied. MN test is known to detect agents that modify chromosome structure and segregation in such a way as to lead to induction of MN (acentric chromosome fragments) in interphase cells. Treatment of cultures with cytochalasin B, an inhibitor of actin polymerization, results in the "trapping" of cells at the binucleate stage where they can be easily identified.

Cultures of the KCL-22 cell line 24 h after sub-culturing were exposed to materials' extracts. 24 h later cytochalasin B (Sigma–Aldrich) dissolved in ethanol was added (not more than 10 μl ethanol per 1 ml of the medium so as not to affect the cell

Table 2
Decomposition temperatures of additives, combustion temperature (T_c) and phase composition of products for the 17%Ni + 83%Zr + additive mixtures.

Additive	Decomposition temperature of additive (°C)	β (wt.%)				Phase composition of products
		0	0.5	0.75	5	
		T_c (°C)				
ZrH_2	500–850	950	930	–	–	Zr, Ni and $Ni_{10}Zr_7$
$CaCO_3$	820–850		–	1130	1500	Zr, NiZr, $Ni_{10}Zr_7$, ZrC, ZrO_2, and $CaZrO_3$
NH_4F	210–250		–	1000	–	Zr, Ni, $Ni_{10}Zr_7$ and traces of ZrN
Teflon	500–650		–	1290	1600	Zr, NiZr, $Ni_{10}Zr_7$ and ZrC

viability and growth) to the final concentration 3 μg ml^{-1}. Cell cultures incubated only with cytochalasin B were used as control. 30 h later the cells were fixed with ethanol: acetic acid (3:1), spread on slides, air dried, and stained with Giemsa (Sigma–Aldrich).

One thousand cells per triplicate cell cultures were scored to assess the frequency (in percent to the control) of cells with one, two, or more nuclei. The cytokinesis-block proliferation index (CBPI) as a measure of cell cycle delay was expressed as: CBPI = [number of binucleate cells + 2 (number of multinucleate cells)]/(total number of cells).

The number of binucleate cells with MN was counted in 1000 binucleate cells in the same cultures. Only micronuclei not exceeding 1/3 of the main nucleus diameter, not overlapping with the main nucleus, and with distinct borders were included in the scoring [38].

The results were statistically treated with the Student's one-tail *t* test.

3. Results

3.1. Reaction in the [17%Ni + 83%Zr] + β% additive systems

It is shown that self-oscillating combustion wave propagates throughout the samples prepared from $(100-\alpha)$%Ni + α%Zr mixtures only in a narrow range of α value ($80 \le \alpha \le 85$). The measured reaction temperature for these samples is in the range 930–980 °C. XRD patterns suggest that the reaction products mainly contain zirconium, nickel and some amount of $Ni_{10}Zr_7$ intermetallic compound. SEM analysis shows that the products consist of fine particles interspersed with molten areas (for XRD pattern and SEM micrograph see Sections 3.2 and 3.3).

The increment of molten phase fraction in a product could be achieved by the increase in combustion temperature due to adding appropriate additives to the initial mixture of reagents. To obtain porous materials it is desirable to use additives which act also as foaming agents. In this study the influence of ZrH_2, $CaCO_3$, NH_4F and Teflon on the combustion parameters and products' features are investigated in the 17%Ni + 83%Zr mixture where zirconium is used as a fine powder. This mixture was selected as it provides the deep eutectic temperature (960 °C, Fig. 3).

Firstly, thermal behavior of additives used is studied by the DTA technique. Decomposition temperature ranges for additives are presented in Table 2. According to the DTG trace, slow decomposition of ZrH_2 starts at 500 °C, then accelerates and completes at 850 °C. Two endothermic peaks corresponding to 550 and 800 °C are observed on the DTA trace. The decomposition temperature range for $CaCO_3$ is relatively narrow (820–850 °C). For NH_4F this range is found to be 210–250 °C. In the case of Teflon a single-stage decomposition starts at 500 °C and ends at 650 °C.

Combustion experiments show that in the [17%Ni + 83%Zr] + β%ZrH_2 system increasing ZrH_2 amount results in a fall in the combustion temperature (Table 2). The combustion limit is observed at $\beta = 0.75$. This additive practically does not change the phase composition of the products.

In [17%Ni + 83%Zr] + β%$CaCO_3$ system the addition of $CaCO_3$ from 0.75 to 5 wt.% increases the combustion temperature from 950 to 1500 °C (Table 2). The analysis of products' microstructure demonstrated that only local molten areas are present (not shown). The samples contain Zr, NiZr, $Ni_{10}Zr_7$, ZrO_2, ZrC and $CaZrO_3$. In spite of high reaction temperatures, the formation of significant amounts of highly refractory compounds ($CaZrO_3$, ZrC and ZrO_2) reduces the fraction of molten intermetallic phases, thus preventing the coalescence of molten areas.

It is revealed that NH_4F is not an appropriate additive to obtain NiZr-based materials due to relatively low decomposition temperature (Table 2). It moves away from the non-reacted part of samples prior to the front propagation. At the same time, exothermic interaction may be suddenly initiated during the mixing of additive with metal powders that means the reaction is not controllable.

The application of Teflon as an additive allows increasing the combustion temperature (Table 2). Teflon provides forming of entirely molten porous products (see the Section 3.3) containing Zr, NiZr, $Ni_{10}Zr_7$, and ZrC.

Thus, in the Ni–Zr system among the additives studied the most suitable one to stimulate the combustion reaction is shown to be Teflon. It acts both as a combustion promoter and foaming agent. In subsequent experiments Teflon is used as an additive.

3.2. Reaction in the Ni–Zr–Teflon system

To determine the influence of α value on combustion parameters the reaction in $[(100-\alpha)$%Ni + α%Zr] + 1.5%Teflon mixtures was investigated at 0.5 MPa. All experiments were performed with fine zirconium powder. It is shown that increasing in α value from 35 to 85 wt.% leads to the combustion temperature rise from 1050 to 1420 °C (Fig. 4). Further increase in α value results in decrease of T_c to 1200 °C. The combustion front velocity monotonously

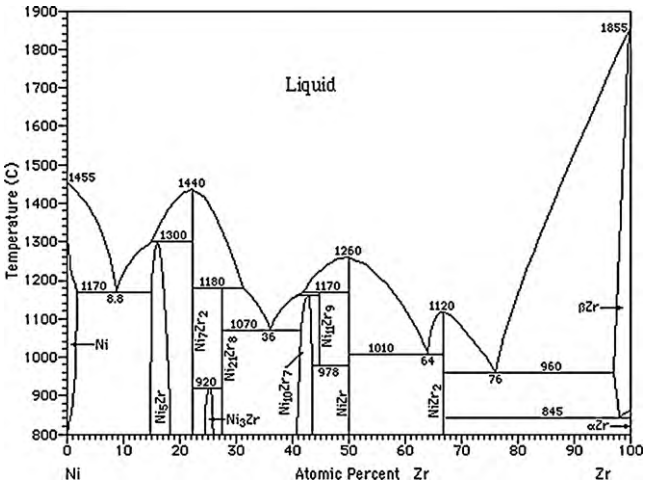

Fig. 3. Binary phase-diagram of the Ni–Zr system.

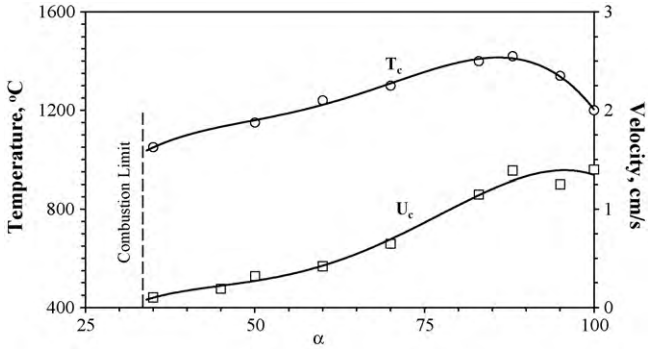

Fig. 4. Combustion temperature and velocity *vs.* α value for the [$(100-\alpha)$Ni + α%Zr] + 1.5%Teflon mixtures, P(Ar) = 0.5 MPa.

increases about 14 times in the range $35 < \alpha < 85$ reaching 1.4 cm s^{-1} at maximum α value. Further increment of α to 100 wt.% does not practically change the combustion front propagation velocity.

The so-called lower combustion limit is observed at $\alpha = 35$ wt.% (Fig. 4). Consequently, the reaction in the mixtures containing zirconium less than 35 wt.% produces no enough heat to sustain the combustion wave. At the same time, the upper combustion limit is not observed, which means that even Ni-free mixture ($\alpha = 100$ wt.%) is able to react in self-sustaining mode. Hence, the following reaction is thought to be responsible for combustion wave propagation:

$$Zr + (C_2F_4)_n \rightarrow ZrC + ZrF_4$$

This reaction is confirmed by the results of DTA analysis in Zr + Teflon and Ni + Teflon mixtures. Very strong exothermic interaction is shown to occur in Zr + Teflon mixture at 550 °C leading to formation of a product containing Zr and ZrC, while in the Ni + Teflon mixture only endothermic effect of polymer decomposition is observed. The possibility of NiF_2 formation as a by-product is not excluded.

The combustion process is observed to be accompanied with release of a white compound (precipitated on the reactor walls) identified as ZrF_4. As this compound is volatile (temperature of sublimation is 910 °C) at reaction temperatures (1000–1400 °C) it can be proposed that it is mainly removed from the melt.

Other important factor influencing on the process conditions and characteristics of materials obtained is the amount of the additive. Increasing in the amount of Teflon to 5 wt.% leads to growth of the combustion velocity (from 0.15 to 1.6 cm s^{-1}) and reaction temperature (from 960 to 1600 °C) (Fig. 5).

XRD patterns for the 17%Ni + 83%Zr initial mixture ($\beta = 0$) and the product formed are shown to be almost identical (Fig. 6a and b). Diffraction lines of Zr, Ni, small lines of $Ni_{10}Zr_7$ intermetallic phase and several non-identified lines are observed in the product (Fig. 6b). Addition of even low amount ($\beta = 0.75$) of Teflon leads

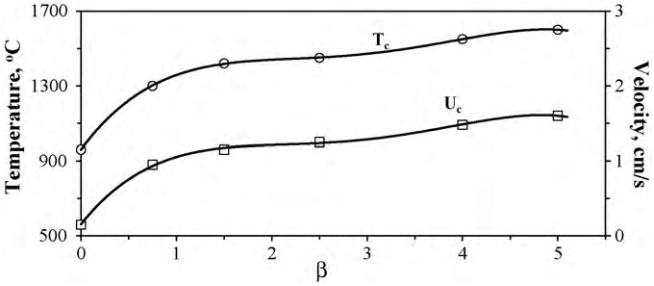

Fig. 5. Combustion temperature and velocity *vs.* β value for the [17Ni% + 83%Zr] + β%Teflon mixtures, P(Ar) = 0.5 MPa.

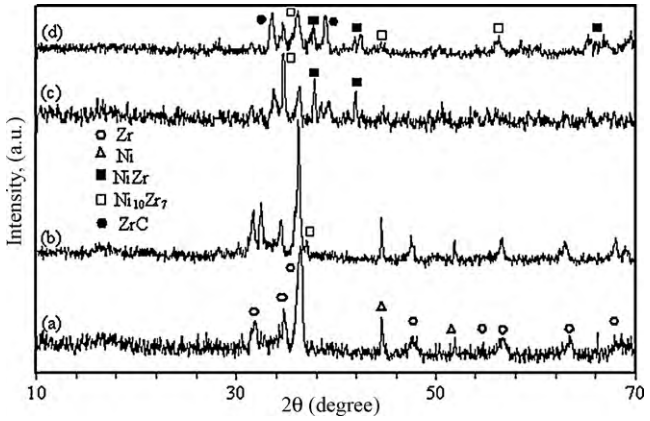

Fig. 6. XRD patterns of 17%Ni + 83%Zr initial mixture (a) and reacted samples at $\beta = 0$ (b), $\beta = 0.75$ (c), $\beta = 4$ (d).

to drastic changes in the product's phase composition (Fig. 6c). In particular, the intensity of Zr diffraction lines significantly decrease and their positions shift. Simultaneously, the diffraction lines of Ni disappear. The product contains NiZr and $Ni_{10}Zr_7$ intermetallic phases and ZrC. Main difference between the products obtained at $\beta = 4$ and $\beta = 0.75$ is found to be the higher intensities of diffraction lines for ZrC (Fig. 6d) at $\beta = 4$.

3.3. Structure of materials

The unstable (oscillating) self-sustaining interaction in the additive-free 17%Ni + 83%Zr mixture forms products with laminated structure (Fig. 7a). Typical SEM micrograph of the product is presented (Fig. 7b). The product is seen to contain fine particles and molten areas. The general porosity of the product is low (about 35%). It should be noted that Teflon strongly affects the product porosity and structure of materials. For example, products of the [$(100-\alpha)$%Ni + α%Zr] + 1.5% Teflon mixtures are fully melted at $70\% < \alpha < 95\%$ range. At 4 wt.% Teflon contents (83%Zr + 17%Ni mixture) the porosity of samples increases up to 55% (Table 3).

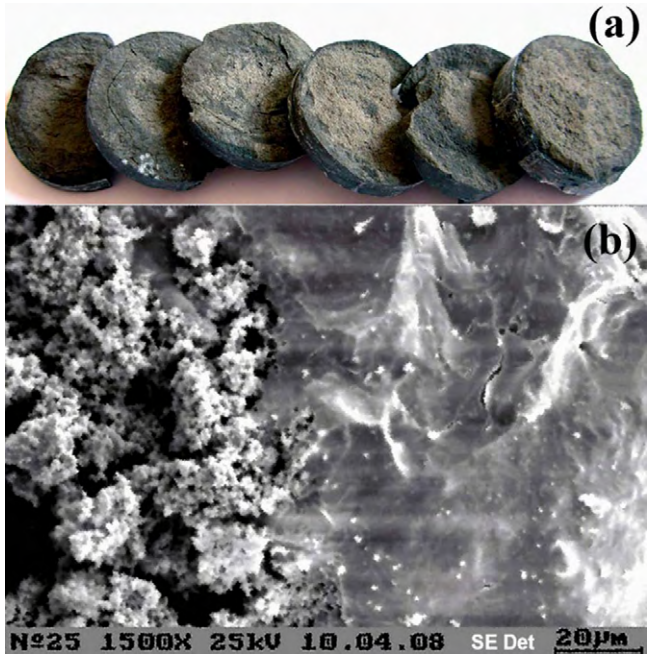

Fig. 7. Photograph of laminated reacted sample (a) made from initial 17Ni% + 83%Zr mixture and its microstructure (b).

Table 3
Effect of Teflon amount (β), gas pressure (P) and zirconium particle size on the general porosity (π) of products.

β (%)	P(Ar) (MPa)	Coarse/fine Zr powders mass ratio	π (%)
0	0.5	0/100	35 ± 2
0.75	0.5	0/100	43 ± 3
4	0.5	0/100	55 ± 2
4	0.1	0/100	60 ± 1
4	1	0/100	55 ± 2
4	0.5	50/50	65 ± 2

Another factor influencing on the combustion features (the velocity and frequency of combustion wave oscillation) and porosity of products is revealed to be the inert gas pressure. Increasing in the pressure from 0.1 to 1 MPa results in threefold growth of U_c (at β = 4%), while the frequency of oscillation (ν) grows from 2 to 25 s^{-1}. These changes take place under practically constant combustion temperature (1550–1600 °C). At the pressure 0.1 MPa ($\nu \sim 2\ s^{-1}$) elongated and open pores are formed (Fig. 8a). The samples have layered structure and the width of each layer corresponds to that of elongated pore. The layered structure is due to oscillating nature of combustion wave propagation. Thus, oscillations contribute to the pore formation. The general porosity of products is about 60% (Table 3). The increase in the pressure to 1 MPa ($\nu \sim 25\ s^{-1}$) results in formation of small narrow pores (Fig. 8b) and the decrease in porosity of product to 55% (Table 3).

It is established experimentally that particle size of the initial reagents is another important factor influencing the combustion features and the structure of products. Partial substitution of fine initial zirconium powder (particle size 5–10 μm) by the coarse one (150–200 μm) in the Teflon-containing mixture (β = 4%) results in decreasing in combustion parameters (gas pressure 0.5 MPa). Furthermore, a combustion limit appears in the case of coarse/fine zirconium powder's mass ratio of 60/40. SEM micrograph of the product synthesized at the 20/80 ratio of zirconium powders show (Fig. 9a) that pores are more elongated and have size 200–500 μm. Increasing the fraction of coarse powder (50/50 ratio) leads to the formation of more spherical pores with dimensions 100–500 μm (Fig. 9b and c). Significant increase in the general porosity (from 55% to 65%) is also registered if coarse/fine powders mass ratio grows to 50/50 (see in Table 3).

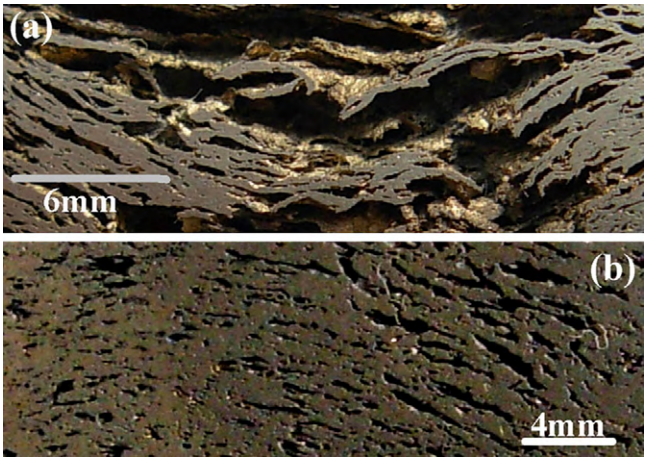

Fig. 8. Photographs of cross-sections of NiZr-based materials, (a) $\nu \sim 2\ s^{-1}$, P(Ar) = 0.1 MPa and (b) $\nu \sim 25\ s^{-1}$, P(Ar) = 1 MPa.

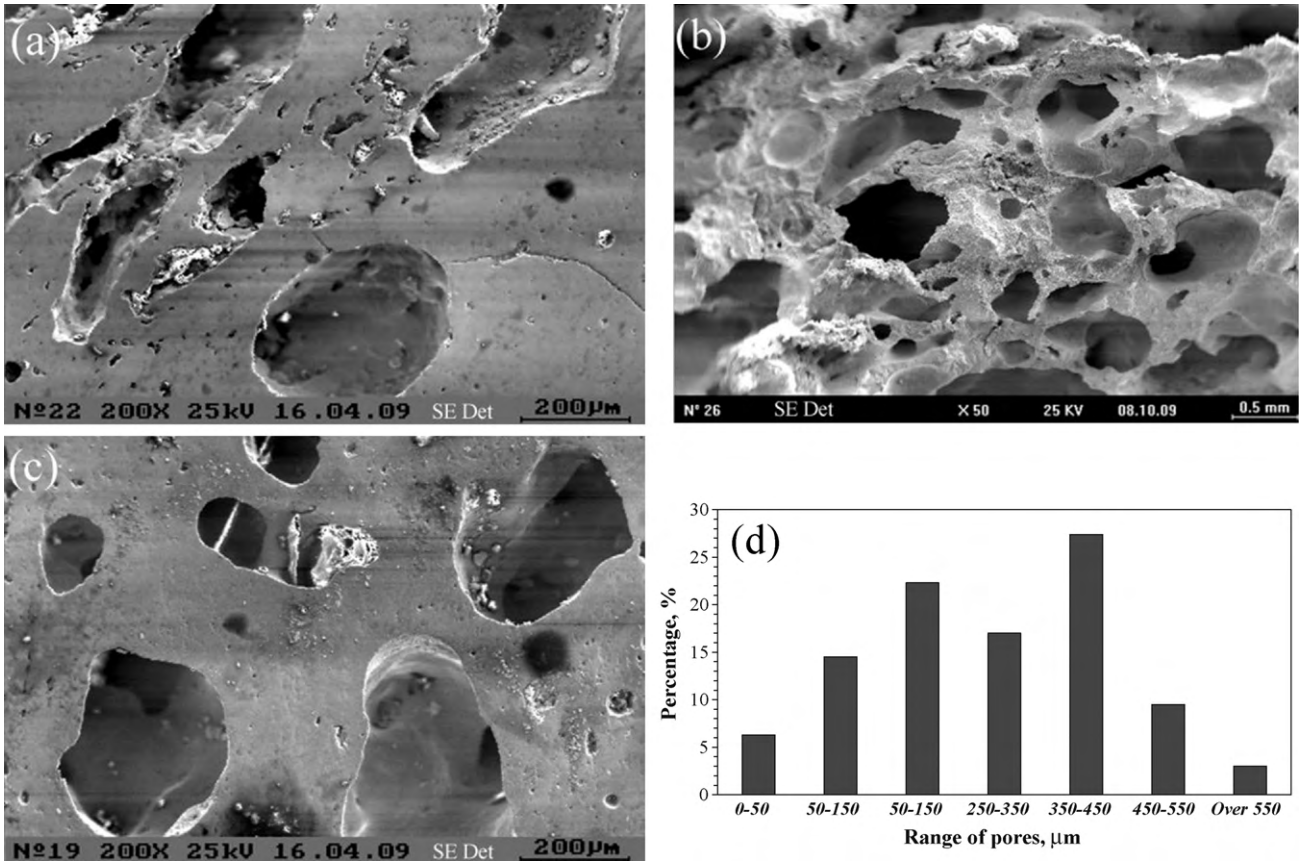

Fig. 9. SEM analyses for NiZr-based materials obtained at coarse/fine zirconium powder ratios 20/80 (a) and 50/50 (b – fracture image, c – polished sample, d – pore size distribution).

Table 4
Concentration of main ions in water extracts of materials.

Duration of extraction (days)	Concentration (mg l^{-1})						
	Fe	Zn	Cu	Ni	Zr	F^-	NO_3^-
1	0.0474	0.0145	0.0123	1.3703	0.1231	1.2307	0.1279
4	0.0271	0.0039	0.0060	0.3741	0.0249	0.1055	0.097

Statistical analysis reveals that about 90% of the pore sizes are in the range of 50–550 μm in the material with 65% porosity (Fig. 9d).

3.4. *In vitro* cytotoxicity of porous NiZr materials

Water extraction experiments of materials obtained have shown that they contain water-soluble components. The main ions detected in the extracts are presented in Table 4; concentrations of others are negligible (not shown). The results suggest that water-soluble compounds can be effectively removed from materials by water extraction. For example, the concentration of Ni ion drops from 1.37 mg l^{-1} after the first extraction to 0.3741 mg l^{-1} after the forth one. Concentrations of other main ions also decrease (Table 4).

The cytotoxicity of obtained NiZr-based materials was tested *in vitro* as a function of Teflon content in the initial [17%Ni + 83%Zr] + β%Teflon mixture. The porosity of tested materials is 45–65%. Extracts of materials incubated with the growth medium for the first time are observed to change the HeLa cell culture morphology (not shown) and provoke intense cell death (Fig. 10a). Subsequent extractions of the same materials appreciably decrease their cytotoxicity (Fig. 10b and c) and after fourth extraction procedure all the materials express no toxicity even for highly sensitive KCL-22 cell line (Fig. 10d). Materials obtained at β = 0.75 and 2.5 become non-toxic after the very first extraction procedure. At higher β values (4 or 5) they become non-toxic only after the fourth extraction.

It is safe to conclude that as-fabricated materials contain cytotoxic components (e.g., NiF_2 and ZrF_4). These compounds can be dissolved in and eluted, at least partly, by the aqueous solvent applied (the growth medium). In that way their levels in the materials is possible to lower to concentrations that are non-toxic for cells *in vitro*.

3.5. Genotoxicity and cell cycle effects

Non-cytotoxic extracts of materials after the fourth extraction are used in these experiments. The numbers of binucleate KCL-22 cells bearing MN in cultures treated with extracts of materials formed at β = 0.75, 2.5, 4 and 5 are 11 ± 3.6; 3 ± 1.7; 3 ± 0, and 7 ± 2.7 per mille, respectively. The differences between these and control (6 ± 1.7) values are insignificant. Thus, the extracts are shown not to raise the MN frequency and have no genotoxic activity.

The same extracts do not change the number of binucleate cells (Fig. 11) and CBPI (not shown). In other words, they have no any side effect on the cell proliferation rate and passing of cells through the cell cycle.

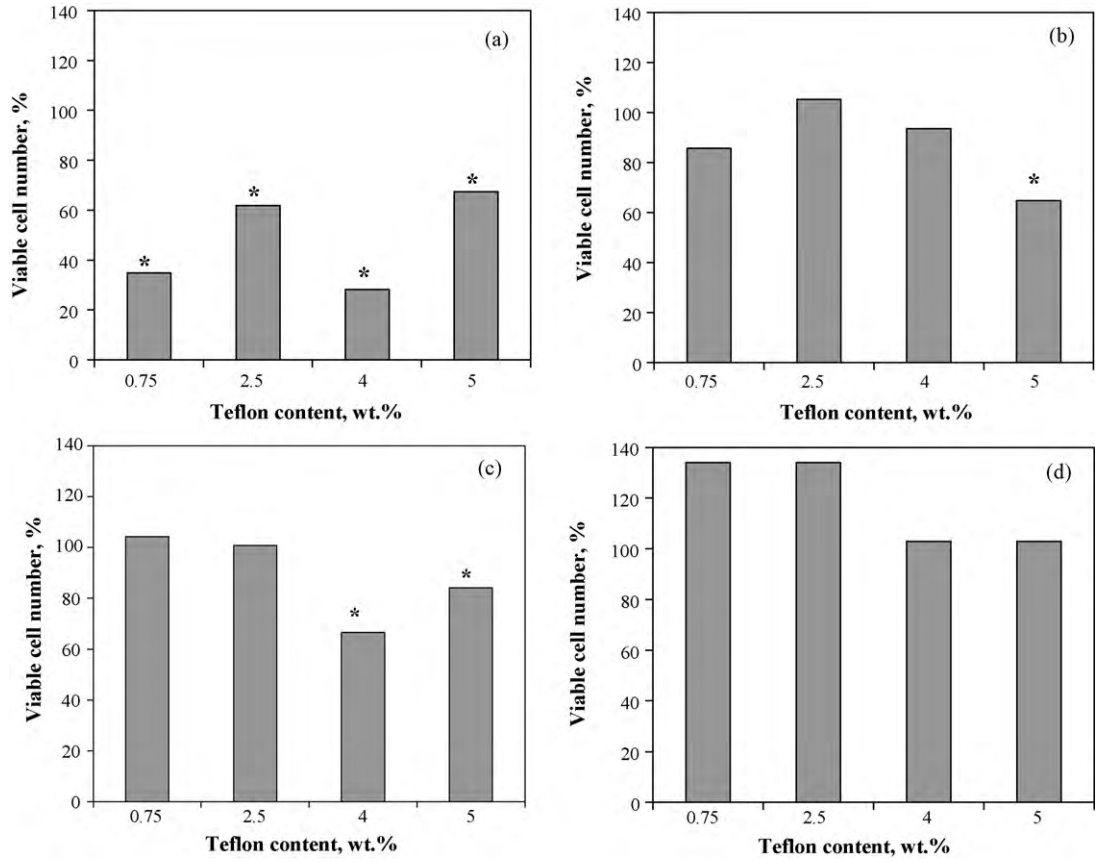

Fig. 10. Cytotoxicity of materials' extracts for HeLa (a, b, and c) and KCL-22 (d) cell lines after the first (a), second (b), third (c) and fourth (d) extractions. *Asterisks indicate values significantly different from the controls.*

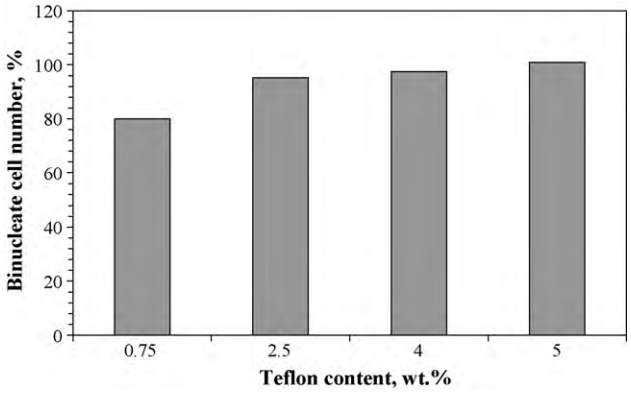

Fig. 11. Effect of materials' extracts on the proliferation rate of KCL-22 cells.

4. Discussion

The present work contributes to our knowledge on *in situ* stimulation of combustion reaction in low-caloric systems and formation of porous NiZr-based intermetallic products. The results obtained in this study and literature data [12–19,25,26] show that some intermetallics cannot be formed under the combustion synthesis regime because of low thermal characteristics of the metals mixture. Two approaches to stimulate low-caloric reactions of such kind are conventional. The first one is external heating of initial mixture before the ignition [12–16] that complicates the technology. The alternative is usage of additives able to initiate and support a parallel exothermic reaction [17,18,27,28]. Adding of foaming agents is also needed at this case to create pores within a product [19,29].

In the work presented new NiZr-based materials were synthesized by CS process without external heating of the reagents. The aptitude of four additives (ZrH_2, $CaCO_3$, NH_4F, and $(C_2F_4)_n$) was tested. Most of these compounds contain elements (O, C, N, and F) possessing high affinity to the initial metallic reagent (i.e., zirconium), they thought to be able to form by-products having high enthalpy of formation (ZrO_2, ZrC, ZrN, ZrF_4, *etc.*) and stimulate self-sustaining reactions.

Hydrides of transition metals were earlier recommended [25,29] as additives providing the formation of intermetallic materials with desired porosity. Our results (Table 2), however, suggest that zirconium hydride is not a suitable agent to synthesize NiZr-based materials as its addition leads to drastic change in the reaction thermal regime and causes so-called combustion limit.

Calcium carbonate does raise the combustion temperature in the Ni + Zr mixture. At the same time CO_2 and CaO obtained in the process of carbonate decomposition react with metallic zirconium forming highly refractory compounds according to the following reactions:

$$Zr + CO_2 \rightarrow ZrC + ZrO_2$$

$$ZrO_2 + CaO \rightarrow CaZrO_3$$

These compounds do not fuse at the reaction temperature; they reduce the fraction of molten intermetallic phase and prevent the coalescence of molten areas. As to ammonia fluoride, it has too low decomposition temperature (Table 2) to be a potential additive. Moreover, this substance is not suitable by safety reasons.

The reaction of zirconium with added Teflon yields ZrC and ZrF_4 (Table 2), the compounds having high enthalpy of formation. Adding of Teflon increases the temperature in the reaction zone up to 1600 °C. The heat generated provides formation of melted NiZr (T_{melt} = 1260 °C) and $Ni_{10}Zr_7$ (T_{melt} = 1170 °C) phases. ZrF_4 at the reaction temperatures (1100–1600 °C) is in gaseous state and acts as a foaming agent. The process conditions in the Ni + Zr + Teflon system are shown (Sections 3.2 and 3.3) to be regulated by Teflon amount, ambient gas pressure and size of reagent (zirconium) particles. Controlling the combustion wave features (temperature, velocity and oscillation frequency) by these factors allows adjusting the phase composition and structure of products. As a result, zirconium carbide containing porous NiZr-based material with desired porosity and pore size distribution was obtained. Carbides of transition metals (e.g., TiC, ZrC) have been widely used in the orthopaedic materials as reinforcing components or biologically inert coatings [17,18,22,39]. These carbides are biocompatible and relatively resistant to body fluid corrosion.

According to the above-stated, the basic criteria can be formulated to select potential additives:

- additive should stimulate the combustion process by increasing the reaction temperature;
- it should have high decomposition temperature;
- it should form suitable solid by-products and gaseous product contributing to the pore formation.

The as-fabricated materials are found to be cytotoxic for human cell lines *in vitro* and become less toxic after washing with water and aqueous solution (the growth medium, Fig. 9). Toxic components are thought to be fluorine derivatives, most likely NiF_2 and ZrF_4, as cytotoxicity level of products is dependent on Teflon contents in the initial reagent mixtures (Section 3.4). As the water-soluble compounds containing detected ions (Table 4) can be toxic for cells and tissues, they should be washed away before application of materials. The materials themselves, after extraction of toxic components, are non-genotoxic and have no effect on the cell proliferation rate.

It is proposed in the future to continue the investigation of biocompatibility of novel porous NiZr-based materials. Particularly, their corrosion resistance and ability of materials to provide cell ingrowth will be investigated.

5. Conclusions

The present study contributes to the key knowledge of *in situ* chemical activation of combustion reaction in low-caloric systems like Ni–Zr and structure formation of porous potential biomaterials. The following results should be summarized:

- The most suitable chemical activator for stimulating combustion reaction in the low-caloric reacting systems like Ni–Zr yielding porous material is Teflon which enables to stimulate the reaction via the formation of gaseous and solid compounds with high specific heat.
- Main factors influencing the combustion conditions in the Ni–Zr–Teflon mixtures are found to be the ratio of metals in the reacting mixture, amount of Teflon, particle size of reagents and ambient gas pressure.
- The obtained porous NiZr-based material contains toxic compounds that may be removed by water extraction procedures; they are not cyto- and genotoxic by themselves and have no effect on the cell proliferation.

Acknowledgements

The authors would like to thank for the financial support provided by the Armenian National Science and Education Fund (ANSEF Project No. EN-matsc-646), State Committee of Science (SCS) of Armenia (Project No. 354), Joint Project No ECSP-09-13/B40 of National Foundation for Science and Advanced Technology

(NFSAT), State Committee of Science (SCS) of Armenia and USA Civilian Research and Development Foundation (CRDF).

Authors are grateful to Dr. T. Liehr (Institute of Human Genetics and Anthropology, Germany) for providing HeLa and KCL-22 cell lines, to Dr. O. Niazyan, Ms. Y. Grigoryan and Mrs. K. Asatryan (Institute of Chemical Physics, NAS of Armenia) for DTA/DTG and microstructural analyses.

References

[1] G. Ryan, A. Pandit, D.P. Apatsidis, Fabrication methods of porous metals for use in orthopaedic applications, Biomaterials 27 (2006) 2651–2670.
[2] M.P. Staiger, A.M. Pietak, J. Huadmai, G. Dias, Magnesium and its alloys as orthopedic biomaterials: a review, Biomaterials 27 (2006) 1728–1734.
[3] J.P. Li, J.R. Wijn, C.A.V. Blitterswijk, K. Groot, Porous Ti6Al4V scaffold directly fabricating by rapid prototyping: preparation and *in vitro* experiment, Biomaterials 27 (2006) 1223–1235.
[4] B.D. Ratner, A.S. Hoffman, F.J. Schoen, J.E. Lemons, Biomaterials Science. An Introduction to Materials in Medicine, second ed., Elsevier Academic Press, San Diego, 2004.
[5] D.F. Williams, On the mechanism of biocompatibility, Biomaterials 29 (2008) 2941–2953.
[6] G. Hunter, V. Pawar, Oxidized zirconium on a porous structure for bone implant use, US patent No. 6,974,625 B2, 2005.
[7] V. Good, K. Widding, G. Hunter, D. Heuer, Oxidized zirconium: a potentially longer lasting hip implant, Mater. Design 26 (2005) 618–622.
[8] G. Hunter, A. Mishra, Prosthetic devices employing contacting oxidized zirconium surfaces, US Patent No. 6,726,725, 2004.
[9] T.B. Massalski, H. Okamoto, P.R. Subramanian, L. Kacprzak, Binary Alloy Phase Diagrams, second ed., ASM Int., Materials Park, OH, 1990.
[10] A.G. Merzhanov, Combustion processes that synthesize materials, J. Mater. Process. Technol. 56 (1996) 222–241.
[11] Z.A. Munir, U. Anselmi-Tamburini, Self-propagating exothermic reactions: the synthesis of high-temperature materials by combustion, Mater. Sci. Rep. 3 (1989) 227–365.
[12] A. Bansiddhi, T.D. Sargeant, S.I. Stupp, D.C. Dunand, Porous NiTi for bone implants: a review, Acta Biomater. 4 (2008) 773–782.
[13] B.Y. Li, L.J. Rong, Y.Y. Li, V.E. Gjunther, Synthesis of porous Ni–Ti shape-memory alloys by self-propagating high-temperature synthesis: reaction mechanism and anisotropy in pore structure, Acta Mater. 48 (2000) 3895–3904.
[14] C.L. Chu, C.Y. Chung, P.H. Lin, S.D. Wang, Fabrication and properties of porous NiTi shape memory alloys for heavy load-bearing medical applications, J. Mater. Process. Technol. 169 (2005) 103–107.
[15] C.W. Goh, Y.W. Gu, C.S. Lim, B.Y. Tay, Influence of nanocrystalline Ni–Ti reaction agent on self-propagating high-temperature synthesized porous NiTi, Intermetallics 15 (2007) 461–467.
[16] A. Biswas, Porous NiTi by thermal explosion mode of SHS: processing, mechanism and generation of single phase microstructure, Acta Mater. 53 (2005) 1415–1425.
[17] R.A. Ayers, D.E. Burkes, G. Gottoli, H. Yi, F. Zhim, L. Yahia, J.J. Moore, Combustion synthesis of porous biomaterials, J. Biomed. Mater. Res. 81A (2006) 634–643.
[18] D.E. Burkes, G. Gottoli, J.J. Moore, Mechanical properties of porous combustion synthesized Ni_3Ti–TiC_x composites, Compos. Sci. Technol. 66 (2006) 1931–1940.
[19] D.E. Burkes, J. Milwid, G. Gottoli, J.J. Moore, Effects of calcium nitride and calcium carbonate gasifying agents on the porosity of Ni_3Ti–TiC composites produced by combustion synthesis, J. Mater. Sci. 41 (2006) 7944–7953.
[20] Y. Han, S. Li, X. Wang, X. Chen, Synthesis and sintering of nanocrystalline hydroxyapatite powders by citric acid sol–gel combustion method, Mater. Res. Bull. 39 (2004) 25–32.
[21] B. Li, A. Mukasyan, A. Varma, Combustion synthesis of CoCrMo orthopedic implant alloys: microstructure and properties, Mat. Res. Innovat. 7 (2003) 245–252.
[22] D.V. Shtansky, N.A. Gloushankova, A.N. Sheveiko, M.A. Kharitonova, T.G. Moizhess, E.A. Levashov, F. Rossi, Design, characterization and testing of Ti-based multicomponent coatings for load-bearing medical applications, Biomaterials 26 (2005) 2909–2924.
[23] H. Jin, Y. Yang, Y. Chen, Z. Lin, J. Li, Mechanochemical-activation-assisted combustion synthesis of α-Si_3N_4, J. Am. Ceram. Soc. 89 (2006) 1099–1102.
[24] V. Rosenband, A. Gany, Activated self-propagating high-temperature synthesis of aluminum and titanium nitrides, Exp. Therm. Fluid. Sci. 31 (2007) 461–467.
[25] L.E. Vardumyan, H.L. Khachatrya, A.B. Harutyunyan, S.L. Kharatyan, Combustion synthesis of TiSi-based intermetallic foams using complex foaming agents, J. Alloy Compd. 454 (2008) 389–393.
[26] M. Besne, I. Agote, M. Gutierrez, A.R. Sargsyan, S.L. Kharatyan, Study of the SHS synthesis of Ti–Al Foams, Int. J. SHS 13 (2004) 209–218.
[27] S.L. Kharatyan, Kh.V. Manukyan, H.H. Nersisyan, H.L. Khachatryan, Macrokinetic laws of activated combustion during synthesis of composite ceramic powders based on silicon nitride, Int. J. SHS 12 (2003) 19–34.
[28] J.A. Puszynski, H.L. Khachatryan, Kh.V. Manukyan, S.L. Kharatyan, Formation of ceramic nanopowders and composites in a self-sustaining reaction regime, in: NSTI Nanotechnology Conference and Trade Show, NSTI Nanotechnol. 1 (2006) 397–402.
[29] X.M. Pan, H.Y. Zhuang, Effect of TiH_2 on the Microstructres and refining performance of Al–Ti–C master alloy, Mater. Sci. Forum. 561–565 (2007) 329–332.
[30] A. Gennari, C. van den Berge, S. Casati, J. Castell, C. Clemedson, S. Coecke, A. Colombo, et al., Strategies to replace in vivo acute toxicity testing. The report and recommendations of ECVAM Workshop 50, in: ECVAM Workshop 50, Altern. Lab. Anim. 32 (2004) 437–459.
[31] U. Marks, V. Sanding, Drug Testing in vitro: Breakthroughs and Trends in Cell Culture Technology, Viley-VCH Verlag GmbH&Co. KGaA, Weinheim, 2007.
[32] W. Strober, Trypan blue exclusion test of cell viability, Curr. Protoc. Immunol. (1997) Appendix 3B, Available from http://www.scribd.com/doc/6909835/Trypan-Blue-Exclusion-Test-of-Cell-Viability (July 2007).
[33] G. Gasparyan, G. Hovhannisyan, R. Ghazaryan, L. Sahakyan, A. Tovmasyan, R. Grigoryan, et al., *In vitro* testing of cyto- and genotoxicity of new porphyrin water-soluble metal derivatives, Int. J. Toxicol. 26 (2007) 479–502.
[34] M. Fenech, The cytokinesis-block micronucleus technique: a detailed description of the method and its application to genotoxicity studies in human populations, Mutat. Res. 285 (1993) 35–44.
[35] M. Fenech, The advantages and disadvantages of cytokinesis-block micronucleus method, Mutat. Res. 392 (1997) 11–18.
[36] M. Fenech, The *in vitro* micronucleus technique, Mutat. Res. 455 (2000) 81–95.
[37] J.M. Parry, A Proposal for a New OECD Guideline for the in vitro Micronucleus Test, 1998, Available from URL http://www.swan.ac.uk/cget/ejgt/articleMNUKEMS Protocol.htm (July 2007).
[38] J.A. Heddle, A rapid *in vivo* test for chromosomal damage, Mutat. Res. 18 (1973) 187–190.
[39] Z. Zhang, T. Xiao, Coatings, coated articles and method of manufacturing thereof, US Patent, 7,320,799 B2, January 22, 2008.